

SCIENTIFIC REPORTS

OPEN

Pathologic N₀ Status in Clinical T₁N₀M₀ Lung Adenocarcinoma is Predictable by the Solid Component Proportion with Quantitative CT Number Analysis

Meng Li¹, Ning Wu^{1,2}, Li Zhang¹, Wei Sun³, Jianwei Wang¹, Lv Lv¹, Jiansong Ren⁴ & Dongmei Lin³

Correctly predicting pathologic regional node-negative (pN₀) disease in patients with lung cancer before operation may avoid unnecessary mediastinal lymph node dissection (MLND). In this study, we analyze the value of the radiographic and histopathological features of primary tumors for predicting pN₀ status in cT₁N₀M₀ lung adenocarcinoma and to establish an optimal surgical strategy for avoiding MLND in cT₁N₀M₀ lung adenocarcinoma patients. We retrospectively investigated the histopathological and radiographic data of 348 surgically resected cT₁N₀M₀ lung adenocarcinoma patients with systematic lymph node dissection from January 2005 to December 2012. Histopathological features and radiographic features were analyzed. Multivariable analysis was used to identify significant predictors of pN₀ disease. Our results showed that pN₀ disease was detected in 306 patients (87.9%) among the 348 patients with cT₁N₀M₀ lung adenocarcinoma. A decreasing trend of the pN₀ disease proportion was observed with both increasing histological grade and decreased differentiation ($P < 0.001$). In multivariable analysis, the solid component proportion was a significant predictor of pN₀ disease. Among 110 patients with a solid component proportion of no more than 21.3%, mediastinal lymph node involvement was not observed. Patients who meet this criterion may be successfully managed with lung resection without MLND.

Anatomical pulmonary resection in combination with mediastinal lymph node dissection (MLND) or sampling remains the standard surgical approach even for early-stage non-small-cell lung cancer (NSCLC) patients^{1,2}. However, the nodal metastatic rate among early NSCLC patients is not high. The reported nodal metastatic rate is 16% to 29% in early-stage NSCLC patients with a peripheral tumor 3 cm or less in diameter, 15% to 20% in patients with a peripheral tumor 2 cm or less³⁻⁵, and as low as 6.6% in clinical T_{1a}N₀M₀ lung adenocarcinoma patients⁶. Considering the surgical injury, MLND is unnecessary and harmful to patients without mediastinal node involvement^{2,7,8}. Correctly predicting pathologic node-negative (pN₀) disease in patients with NSCLC before operation may avoid unnecessary MLND, although it is an extremely difficult problem in clinical practice. Because the relative low diagnostic sensitivity, these tumors with no nodal involvement on computed tomography (CT) or even positron emission tomography (PET)/CT image, which are staged as clinical N₀ (cN₀) disease, may also have pathological regional lymph node metastases^{9,10}. Consequently, MLND is still adopted as a gold standard in almost NSCLC surgical treatments.

¹Department of Diagnostic Radiology, National Cancer Center/Cancer Hospital, Chinese Academy of Medical Sciences and Peking Union Medical College, Beijing, 100021, China. ²PET-CT center, National Cancer Center/Cancer Hospital, Chinese Academy of Medical Sciences and Peking Union Medical College, Beijing, 100021, China. ³Department of Pathology, Beijing Cancer Hospital, Beijing, 100142, China. ⁴National Office for Cancer Prevention and Control, National Cancer Center/Cancer Hospital, Chinese Academy of Medical Sciences and Peking Union Medical College, Beijing, 100021, China. Correspondence and requests for materials should be addressed to N.W. (email: cjr.wuning@vip.163.com)

Recent advancements in the quality of high-resolution CT (HRCT) and the widespread practice of low-dose CT (LDCT) for lung cancer screening have resulted in a greater increase in the early detection of smaller-sized NSCLC, especially lung adenocarcinoma appearing as subsolid nodule^{11,12}. As a result, limited resection like wedge resection or segmentectomy is more favored and the necessity of standard lobectomy begin to be questioned for small or subsolid types of adenocarcinoma². Meanwhile, the degree to which MLND is necessary also becomes a challenging issue because the biological behavior of small lung adenocarcinomas showing as subsolid nodules on CT is less aggressive and usually pN₀ diseases. These patients are good candidates for the omission of MLND. Therefore, it is very important to establish reliable prediction criteria for pN₀ disease preoperatively especially using quantitative radiographic imaging to avoid performing MLND.

In this study, we attempt to analyze the value of radiographic and histopathological features of primary tumors for predicting pN₀ disease in cT₁N₀M₀ lung adenocarcinoma to establish an optimal surgical strategy for avoiding unnecessary MLND in these patients. We analyzed both HRCT and PET/CT indexes, and we also proposed three-dimensional computer quantified CT number analysis to calculate the solid component (Sc) proportion and ground glass opacity component (GGOc) proportion.

Results

Patient demographics. The clinicopathological characteristics of the 348 patients with lung adenocarcinoma included in this study are summarized in Table 1. Of the 348 patients, 306 (87.9%) had pN₀ disease, and 42 (12.1%) had nodal metastasis. The pN₀ disease proportion was 83.6% (122/146) in males and 91.1% (184/202) in females ($P=0.033$).

Correlation between pN₀ disease proportion and pathological features. The pN₀ disease proportion in histological Grade 1, Grade 2, Grade 3 and Grade 4 was 100%, 97.7%, 82.5% and 73.3%, respectively (Table 2). The pN₀ disease proportion in the well-differentiated group, moderately differentiated group and poorly differentiated group was 97.7%, 80.6% and 65.5%, respectively (Table 3). Decreasing trends were observed for both histological grade and differentiation grade ($P < 0.001$).

Radiographic features analysis. The univariate analysis of radiographic features of node-negative and node-positive disease is presented in Table 4. Tumor size, size stratification, appearance, location, contour, GGOc proportion, Sc proportion and maximum SUV (SUV_{max}) differed significantly between pN₀ disease and node-positive disease ($P=0.002$, $P=0.008$, $P < 0.001$, $P=0.032$, $P=0.006$, $P < 0.001$, $P < 0.001$, $P=0.001$, respectively). Specific to quantitative radiographic indexes, the pN₀ disease had more GGOc proportion, less Sc proportion (Fig. 1) and lower SUV_{max} (Fig. 2).

Logistic regression analysis demonstrated that the Sc proportion was only significant predictor of pN₀ disease ($\beta = 6.153$, $P = 0.001$; $OR = 470.085$, 95% $CI: 12.291 \sim 17978.987$). With the increase of Sc proportion, the chance of pN₀ disease is reduced (Fig. 3). The positive predictive value (PPV) of pN₀ disease was 100% for patients with a tumor Sc proportion of no more than 21.3%. Of the 348 patients, only 137 underwent PET/CT, and thus SUV_{max} was removed from the multivariate analysis.

Discussion

A randomized, prospective clinical trial has suggested that MLND can be avoided if there is sufficient evidence of pN₀ disease¹³. Although multiple studies have attempted to identify clinical, pathological and radiographic factors of lymph node status in early-stage adenocarcinoma^{6,7,14–18}, our study differs from these previous studies in several ways. First, this study made cT₁N₀M₀ lung adenocarcinoma a separate object of study. Second, all resected specimens were reviewed pathologically according to the 2011 IASLC/ATS/ERS classification, and a tumor-grading system was established based on histopathological subtypes according to the newly proposed classification¹⁹. Third and most important, quantitative radiographic analysis method was introduced, the Sc and GGOc proportion calculated using three-dimensional computer-quantified CT number analysis was adopted to qualitatively reflect the tumor internal appearance, resulting in more objective and convenient selection criteria for clinical application.

Our study results included three main findings: (a) the Sc proportion was an independent predictor of pN₀ disease in cT₁N₀M₀ lung adenocarcinoma; (b) all cT₁N₀M₀ lung adenocarcinoma patients with an Sc proportion of no more than 21.3% had no lymph node metastasis; and (c) the pN₀ disease proportion exhibited a decreasing trend with both increasing histological grade and differentiation grade. Our results may have clinical implications. With the aid of preoperative quantitative radiographic features, we differentiated cT₁N₀M₀ lung adenocarcinoma patients with or without pN₀ disease, thus reducing unnecessary MLND.

In our study, tumors were graded according to four classifications based on histopathological subtypes and prognosis. Sica *et al.*²⁰ first proposed a 3-tier grading system for lung adenocarcinoma in 2010: Grade 1, a pattern with low metastatic potential (bronchioloalveolar carcinoma, BAC); Grade 2, patterns with intermediate metastatic potential (acinar and papillary); and Grade 3, patterns with high metastatic potential (solid and micropapillary). However, in 2011, the newly proposed lung adenocarcinoma classification discontinued the use of “BAC”, and other changes in uniform terminology, such as adenocarcinoma *in situ* (AIS) and minimally invasive adenocarcinoma (MIA), and diagnostic criteria were implemented¹⁹. Studies^{21,22} have shown that this new classification system is a stage-independent predictor of survival. Five-year disease-free survival is 100% or near 100% in patients with AIS and MIA, more than 85% in lepidic predominant invasive adenocarcinoma, 65% in acinar and papillary predominant invasive adenocarcinoma, and 40% in solid and micropapillary predominant invasive adenocarcinoma. The tumor-grading system in this study is based on a combination of the classification of Sica *et al.* and the lung adenocarcinoma classification system proposed in 2011. A higher grade represents a worse prognosis.

Characteristics	No. of patient (%)
Median age (y) ^a	58.4 ± 9.8 (31~84)
Sex	
Male	146 (42.0)
Female	202 (58.0)
Smoking status	
Current or former smoker	109 (31.3)
Nonsmoker	239 (58.0)
Invasive lobe	
RUL	139 (39.9)
RML	19 (5.5)
RLL	62 (17.8)
LUL	80 (23.0)
LLL	48 (13.8)
Surgical procedure	
Wedge resection	25 (7.2)
Segmentectomy	1 (0.3)
Lobectomy	322 (92.5)
Imaging technique ^b	
CT	348 (100)
PET/CT	137 (39.4)
Subtype predominance	
AIS	36 (10.3)
MIA	44 (12.6)
Lepidic	43 (12.4)
Acinar	170 (48.9)
Papillary	30 (8.6)
Micropapillary	5 (1.4)
Solide	10 (2.9)
Variants	10 (2.9)
N Stage	
N ₀	306(87.9)
N ₁	21(6.0)
N ₂	21(6.0)
Pathologic Stage	
IA	164 (47.1)
IB	142 (40.8)
IIA	21 (6.0)
IIIA	21 (6.0)

Table 1. Patient characteristics. Note. –Unless otherwise indicated, data are numbers, with percentages in parentheses. ^aData are means ± standard deviations, with range in parentheses. ^bAll patients underwent CT examination. AIS, adenocarcinoma *in situ*; MIA, minimally invasive adenocarcinoma; LLL, left lower lobe; LUL, left upper lobe; RLL, right lower lobe; RML, right middle lobe; RUL, right upper lobe.

Tumor grades	pN ₀ disease proportion	P
Grade 1	80/80 (100%)	<0.001
Grade 2	42/43 (97.7%)	
Grade 3	165/200 (82.5%)	
Grade 4	11/15 (73.3%)	
Total	298/338 (88.4%)	

Table 2. Trend of pN₀ disease proportion among different tumor grades. Note. – 10 patients with invasive adenocarcinoma of a variant pattern were not included; pN₀, pathologic node-negative.

A decreasing trend in the pN₀ disease proportion with increasing tumor grade and decreasing tumor differentiation was observed in this study, consistent with the worse prognosis of lung adenocarcinoma patients with higher tumor grade and poorer tumor differentiation. In this study, all cT₁N₀M₀ lung adenocarcinoma patients

Tumor differentiation degrees	pN ₀ disease proportion	P
Well-differentiated group	171/175 (97.7%)	<0.001
Moderately differentiated group	116/144 (80.6%)	
Poorly differentiated group	19/29 (65.5%)	
Total	306/348 (87.9%)	

Table 3. Trend of pN₀ disease proportion among different tumor differentiation degrees. Note. – pN₀, pathologic node-negative.

Radiographic features	Node-positive	Node-negative	χ^2/t	P
HRCT	42	306		
Size ^a	2.20 ± 0.51	1.90 ± 0.58	–3.143	0.002
Size stratification			9.556	0.008
≤ 1 cm	0	21		
1–2 cm	17	173		
> 2 cm	25	112		
Appearance				
GGO	0	52	43.980	<0.001
PSN	4	142		
SN	38	112		
Location			4.579	0.032
Center	12	47		
Periphery	30	259		
Contour			10.127	0.006
Smooth	2	67		
Lobular	20	156		
Spiculated	20	86		
Necrosis			1.482	0.223
Yes	6	26		
No	36	280		
Quantified CT number analysis				
GGOc proportion ^a	(5 ± 6) %	(24 ± 25) %	11.522	<0.001
Sc proportion ^a	(82 ± 17) %	(42 ± 32) %	–12.799	<0.001
PET/CT	137	10		
SUV _{max}	5.23 ± 2.71	3.20 ± 2.77	–3.510	0.001

Table 4. Correlation between radiographic features and lymph node status. Note. – Unless otherwise indicated, data are number of patients. ^aData are means ± standard deviation. HRCT, high-resolution computer tomography; GGOc, glass-ground-opacity component; Sc, solid component; PET, positron emission tomography; SUV, standard uptake value.

with grade 1 tumors (AIS or MIA) had pN₀ disease, whereas only 97.7% of patients with well-differentiated tumors had pN₀ disease. Therefore, we believe that tumor grade has stronger predictive ability for lymph node status than tumor differentiation and that tumor grade 1 is a significant predictor of pN₀ disease. However, because of histological heterogeneity, AIS and MIA can only be diagnosed in resected specimens and not in small biopsies or cytology specimens²³. Consequently, histopathological subtypes have limited significance in predicting node metastasis preoperatively and determining the most appropriate surgical procedures.

In univariate analysis of radiographic features, tumor size, size stratification, location, contour, appearance, Sc proportion, GGOc proportion and SUV_{max} were associated with pN₀ disease. In this study, all 21 patients with a tumor size of no more than 1 cm had pN₀ disease, in accordance with previous study¹⁴. We also found that compared with patients with node-positive disease, primary tumors in patients with pN₀ disease are more likely to present a smooth margin and peripheral location. Smooth margin and peripheral location were frequently proven to be benign signs in lung nodule diagnosis. Tumor appearance has been proven to be a significant predictor of lymph node status. Researchers have found that most patients with a dominant GGO component on CT have no lymph node metastasis¹⁵. In this study, all 52 patients with pGGO had pN₀ disease, consistent with previous studies^{6,16}. However, tumor appearance is only used as a subjective and visual characteristic in the past study, and thus is not sufficiently objective and accurate for prediction of pN₀ disease. The great progresses of computer make quantitative imaging increasingly applying in modern radiology practice, assisting in the clinical assessment and providing a source of biomarkers for a spectrum of diseases²⁴. In the current study, the Sc proportion and GGOc proportion calculated by three-dimensional computer-quantified CT number analysis were adopted to qualitatively reflect tumor appearance innovatively, resulting in more objective and accurate selection criteria

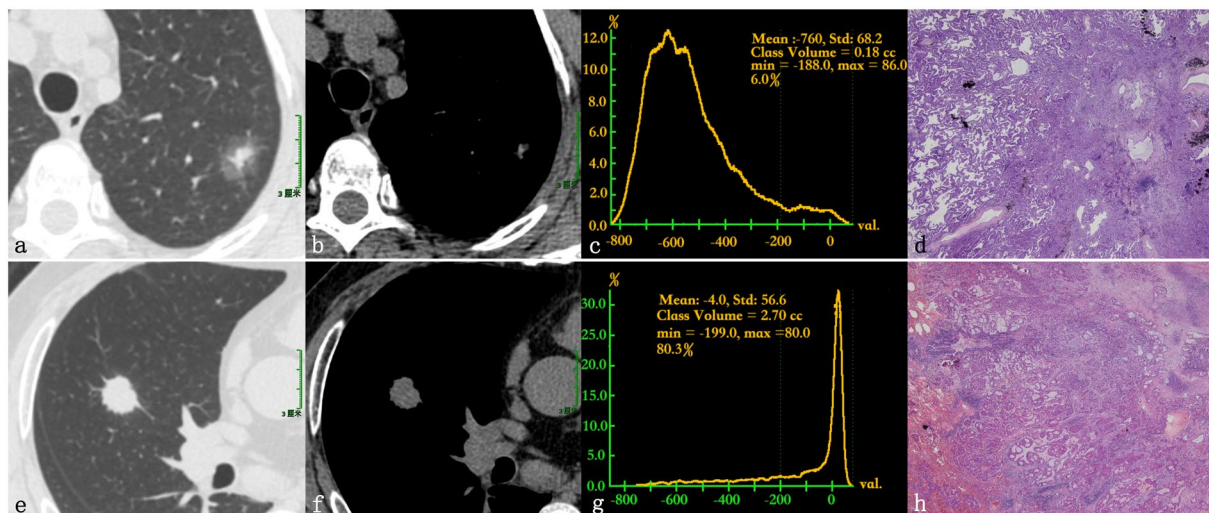


Figure 1. Images of a 59-year-old female patient with invasive adenocarcinoma (a–d) and a 45-year-old male patient with invasive adenocarcinoma (e–h). (a,b) The lung window and mediastinal window of the axial HRCT showed a partially solid nodule in the left upper lobe. (c) The CT number distribution curve revealed that the solid component proportion of the nodule was 6%. (d) The photomicrograph (hematoxylin and eosin staining; magnification $\times 20$) revealed a lepidic-predominant invasive adenocarcinoma consisting of 80% lepidic pattern and 20% acinar pattern (pT₁N₀M₀). (e,f) The lung window and mediastinal window of the axial HRCT showed a solid nodule in the right upper lobe. (g) The CT number distribution curve revealed that the solid component proportion of the nodule was 80.3%. (h) The photomicrograph (hematoxylin and eosin staining; magnification $\times 100$) revealed an acinar-predominant invasive adenocarcinoma consisting of 80% acinar pattern and 20% solid pattern (pT₁N₂M₀, right superior mediastinal lymph node metastasis, 3/6; subcarinal lymph node metastasis, 1/1).

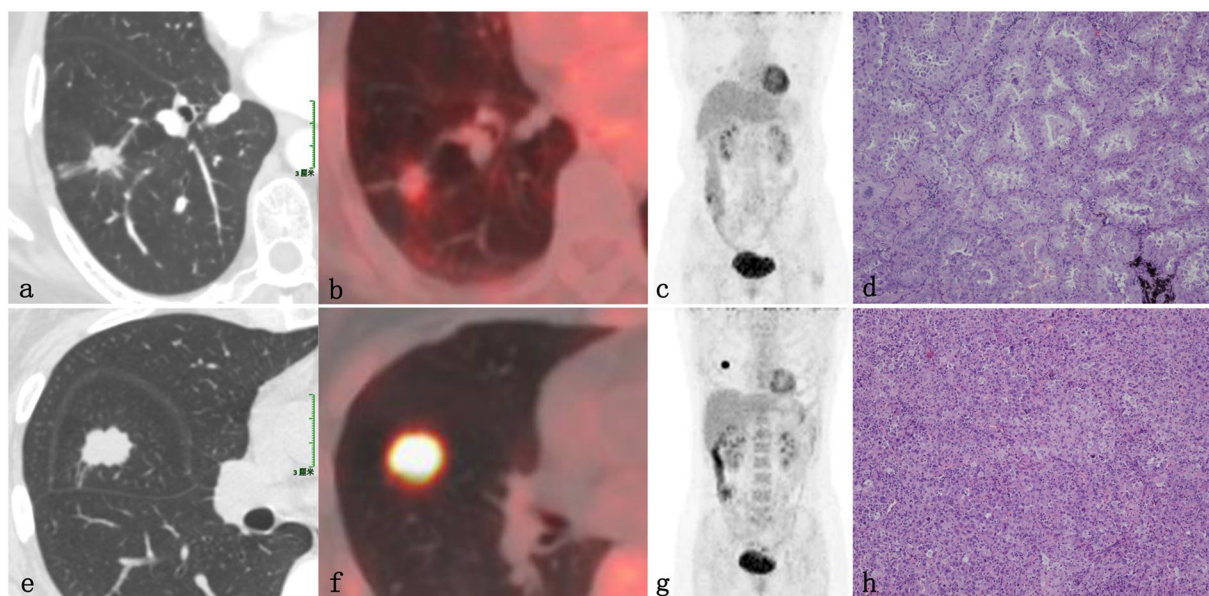


Figure 2. Images of a 59-year-old female patient with invasive adenocarcinoma (a–d) and a 46-year-old female patient with invasive adenocarcinoma (e–h). (a) The lung window of the axial HRCT showed a solid nodule in the right lower lobe. (b) PET/CT revealed low metabolic activity (SUV_{max} 1.5). (c) PET showed no other abnormal FDG uptake in the whole body. (d) The photomicrograph (hematoxylin and eosin staining; magnification $\times 100$) indicated an acinar predominant invasive adenocarcinoma consisting of 60% acinar pattern, 35% lepidic pattern and 5% papillary pattern (pT₁N₀M₀). (e) The lung window of the axial HRCT showed a solid nodule in the right lower lobe; the nodule had a lobulated and speculated margin. (f) PET/CT revealed high metabolic activity (SUV_{max} 7.8). (g) PET showed no other abnormal FDG uptake in the whole body. (h) The photomicrograph (hematoxylin and eosin staining; magnification $\times 100$) indicated a solid predominant invasive adenocarcinoma consisting of 70% solid pattern and 30% acinar pattern (pT₁N₁M₀, parabranchial lymph node metastasis of the right middle lobe, 1/3).

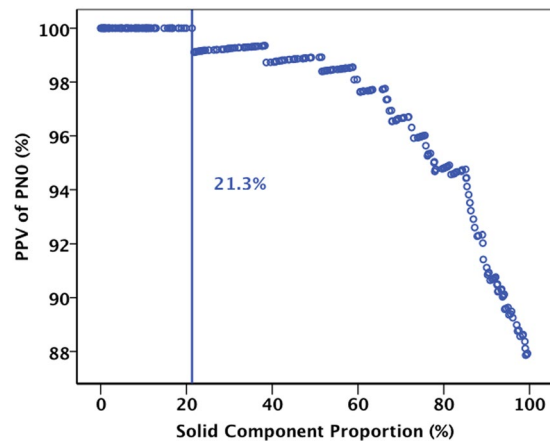


Figure 3. The Positive predictive value (PPV) of pN₀ disease in cT₁N₀M₀ lung carcinoma based on the tumor solid component (Sc) proportion.

for pN₀ disease. The Sc proportion and GGOc proportion were all associated with lymph node status. Primary tumors in patients with pN₀ disease had lower Sc proportions and higher GGOc proportions than patients with node-positive disease. Studies^{7,17,18} have demonstrated that the solid component is a powerful predictor of lymph node metastasis, consistent with our study. SUV_{max} is a semiquantitative index of FDG uptake of PET/CT, which is associated with glucose metabolism in tissue. SUV_{max} was significantly lower in patients with pN₀ disease than patients with node-positive disease in this study, consistent with previous studies^{7,25–27}.

We analyzed all factors except SUV_{max} by logistic multivariate analysis to assess the joint effects and interactions of the variables on pN₀ disease. Our results showed that only the Sc proportion retained statistical significance, whereas tumor size, size stratification, location, contour, appearance and GGOc proportion did not differ significantly in multivariate analysis. We believe that the effects of these factors were substituted by the enrolled index. When Sc proportion ≤21.3% was used as the criterion, the PPV for pN₀ disease was 100%. On the basis of our result, patients of cT₁N₀M₀ lung adenocarcinoma who meet this reliable prediction criterion may omit MLND when surgical treatment.

Our study has several limitations. First, this is a single study; further studies at multiple centers are needed to confirm our results, especially the predictive value of Sc. Second, this is a retrospective study, and a prospective study is needed to verify this conclusion. Finally, we did not perform survival analysis because the follow-up time was too short in some cases; advanced study is warranted to analyze patient survival.

In conclusion, we respectively reviewed 348 cT₁N₀M₀ lung adenocarcinoma patients who underwent surgical pulmonary resection with systematic MLND at our hospital in an attempt to investigate independent predictors of pN₀ disease. The Sc proportion was identified as statistically significant predictive risk factor. The PPV of pN₀ disease was 100% for patients with a tumor Sc proportion of no more than 21.3%. Patients who meet this criterion may be managed with lung resection without MLND.

Materials and Methods

Patients. This prospective study was approved by the institutional review board at the Cancer Hospital of the Chinese Academy of Medical Sciences, and the informed consent was waived due to the retrospective nature of the study and the data were going to be analyzed anonymously. This study was conducted in accordance with the Declaration of Helsinki.

A total of 348 consecutive patients with surgically resected cT₁N₀M₀ lung adenocarcinoma at our hospital between January 2005 and December 2012 were included. The inclusion criteria for our study were as follows: (a) single adenocarcinomas (3 cm or less in diameter at HRCT) with no evidence of malignant satellite nodules (as proven by prior imaging study or lung biopsy); (b) no hilar or mediastinal lymphadenopathy on imaging study or at mediastinoscopy; a short lymph node diameter greater than 1 cm on CT axial image with window level in 380 HU and window within 40 HU or maximum SUV (SUV_{max}) on PET/CT image more than 2.5 was determined as lymphadenopathy; (c) first treatment with surgical pulmonary resection plus systematic MLND (more than 6 hilar or mediastinal lymph nodes resected); (d) either integrated ¹⁸F fluorodeoxyglucose (¹⁸F-FDG) PET/CT or chest HRCT studies acquired within 1 month before resection; (e) both pathological sections and clinical data were available for review.

Imaging and Interpretation. All 348 patients included in this study had undergone chest HRCT for preoperative staging. HRCT images were obtained with an eight- (LightSpeed Ultra, GE Medical Systems), 16- (ProSpeed or Discovery ST, GE Medical Systems) or 64- (LightSpeed VCT, GE Medical Systems or Toshiba Aquilion, TOSHIBA Medical Systems) slice spiral CT scanner. Unenhanced CT images were obtained at 120 kVp and 250–350 mA with a reconstruction kernel with a standard algorithm. The reconstruction thickness was 1.0 or 1.25 mm, and the interval was 0.8 or 1.0 mm. A total of 182 patients underwent enhanced HRCT examination, in which 60 to 80 ml of intravenous contrast was administered at 2.0 to 2.5 mL/s and enhanced images were obtained 25 to 30 seconds after contrast infusion.

HRCT images were assessed retrospectively for morphological features and three-dimensional computer-quantified CT number analysis. Two radiologists (M.L. and L.Z., 11 and 8 years of experience, respectively), who were informed that the involved patients had surgically treated adenocarcinoma but were blinded to histological subtypes, analyzed the morphological features on Carestream GCRIS 2.1 PACS workstation (Carestream Health) in consensus. The morphological features included tumor size (the longest tumor diameter on the transverse lung window image in which the largest nodule dimension appeared), appearance (solid nodule [SN], part-solid nodule [PSN], or pure ground-glass-opacity [pGGO])²⁸, location (center or periphery, periphery was defined as within 3 cm of the pleura)²⁹, and contour (smooth, lobular or spiculated), necrosis (necrosis of tumor was defined as low attenuation in the tumor). Three-dimensional computer-quantified CT number analysis was performed on an ADW 4.6 workstation (GE Medical Systems) to measure the proportion of GGOc and Sc. This measurement was performed in two steps. For the first step, the entire tumor mass was separated from surrounding anatomic structures using computer-aided volume measurement software (Auto Contour in Volume Rendering, GE Medical Systems). The computer generated tumor boundaries were then visually inspected by a radiologist (L.Z.) for accuracy and consistency. If any segmentation results were considered suboptimal, the tumor contours that were superimposed on the original images were edited by the same radiologist (L.Z.), and then the mean CT value of tumor was automatically calculated by computer. Threshold values of GGOc and Sc were obtained by receiver operating characteristic (ROC) curves. As the second step, the entire tumor mass was separated using the same method in the first step, and the computer automatically generated the CT number histogram of the tumor. The proportion of GGOc/Sc was calculated based on the threshold values obtained in the first step. The calculation methods were also described in detail in our previous report³⁰.

Two chest radiologists with PET/CT diagnostic experience prospectively evaluated the integrated PET/CT images. For semiquantitative analysis of ¹⁸F-FDG uptakes, a region of interest (ROI) was placed over the tumor site on the hottest trans-axial slice. In some patients, nodular FDG uptake could not be identified on the PET component images of the PET/CT study. In those patients, a ROI was drawn in a presumed nodular location, taking into account the CT component images of PET/CT. The SUV_{max} within the ROI was used as the reference measurement.

Pathologic Evaluation. All resected specimens were reviewed pathologically by an experienced lung pathologist (S.W., 8 years of experience in lung pathology) according to the 2011 International association for the study of lung cancer/American thoracic society/European respiratory society (IASLC/ATS/ERS) classification¹⁹. For difficult cases, histological subtypes were assessed by consultation with pathological experts. Based on the reported prognosis of lung adenocarcinoma^{31–34}, tumors were graded according to four classifications. Grade 1 included histological subtypes of adenocarcinoma *in situ* (AIS) and minimally invasive adenocarcinoma (MIA). Grade 2 corresponded to the lepidic pattern of invasive adenocarcinoma. Grade 3 corresponded to tumors that showed acinar or papillary patterns. Grade 4 corresponded to tumors that showed micropapillary or solid patterns. When tumors were composed predominantly of a variant pattern, the tumors were removed from this classification system because they were uncommon and heterogeneous in terms of biological behavior and prognosis. Considering the proximity of tumor cells and normal cells under the microscope, tumors were divided into the well-differentiated group, moderately differentiated group and poorly differentiated group.

Statistical analysis. The trends of pN₀ disease proportion among the different tumor grades and tumor differentiation degrees were assessed by chi-square trend test. The prevalences of nominal variables (e.g., tumor appearance, location, contour and intratumoral necrosis) were compared using Fisher's exact test. Differences in the mean values of continuous variables (e.g., tumor size, GGOc proportion, Sc proportion and SUV_{max}) were compared using the Independent-Student's *t* test. Multivariate logistic regression analysis was used to identify significant predictors of pathologic node-negative disease. All statistical analyses were performed using a commercial software package (SPSS, Inc., an IBM Company, Chicago, IL, USA). A *P* value of less than 0.05 was considered to indicate a significant difference.

Data availability. All data generated or analysed during this study are included in this published article (and its Supplementary Information files).

References

- Ginsberg, R. J. & Rubinstein, L. V. Randomized trial of lobectomy versus limited resection for T1 N0 non-small cell lung cancer. Lung Cancer Study Group. *The Annals of thoracic surgery* **60**, 615–622; discussion 622–613 (1995).
- Cho, S. The necessity of mediastinal lymph node resection for screen-diagnosed non-small cell lung cancer (NSCLC) manifesting as subsolid nodule. *J Thorac Dis* **8**, E1079–E1081, <https://doi.org/10.21037/jtd.2016.08.68> (2016).
- Ishida, T. *et al.* Strategy for lymphadenectomy in lung cancer three centimeters or less in diameter. *The Annals of thoracic surgery* **50**, 708–713 (1990).
- Inoue, M. *et al.* Clinicopathologic study of resected, peripheral, small-sized, non-small cell lung cancer tumors of 2 cm or less in diameter: pleural invasion and increase of serum carcinoembryonic antigen level as predictors of nodal involvement. *The Journal of thoracic and cardiovascular surgery* **131**, 988–993, <https://doi.org/10.1016/j.jtcvs.2005.12.035> (2006).
- Bao, F. *et al.* Predictive risk factors for lymph node metastasis in patients with small size non-small cell lung cancer. *Journal of thoracic disease* **6**, 1697–1703, <https://doi.org/10.3978/j.issn.2072-1439.2014.11.05> (2014).
- Ye, B. *et al.* Factors that predict lymph node status in clinical stage T1aN0M0 lung adenocarcinomas. *World J Surg Oncol* **12**, 42, <https://doi.org/10.1186/1477-7819-12-42> (2014).
- Tsutani, Y. *et al.* Prediction of pathologic node-negative clinical stage IA lung adenocarcinoma for optimal candidates undergoing sublobar resection. *The Journal of thoracic and cardiovascular surgery* **144**, 1365–1371, <https://doi.org/10.1016/j.jtcvs.2012.07.012> (2012).

8. Shayani, J., Flores, R. M. & Hakami, A. Mediastinal lymph node dissection: the debate is not resolved. *J Thorac Dis* **9**, 1848–1850, <https://doi.org/10.21037/jtd.2017.06.128> (2017).
9. Li, M. *et al.* Regional nodal staging with 18F-FDG PET-CT in non-small cell lung cancer: Additional diagnostic value of CT attenuation and dual-time-point imaging. *European journal of radiology* **81**, 1886–1890, <https://doi.org/10.1016/j.ejrad.2011.03.074> (2012).
10. Schmidt-Hansen, M. *et al.* PET-CT for assessing mediastinal lymph node involvement in patients with suspected resectable non-small cell lung cancer. *Cochrane Database Syst Rev*, CD009519, <https://doi.org/10.1002/14651858.CD009519.pub2> (2014).
11. Aberle, D. R. *et al.* Reduced lung-cancer mortality with low-dose computed tomographic screening. *The New England journal of medicine* **365**, 395–409, <https://doi.org/10.1056/NEJMoa1102873> (2011).
12. Zhang, L., Li, M., Wu, N. & Chen, Y. Time Trends in Epidemiologic Characteristics and Imaging Features of Lung Adenocarcinoma: A Population Study of 21,113 Cases in China. *PLoS One* **10**, e0136727, <https://doi.org/10.1371/journal.pone.0136727> (2015).
13. Allen, M. S. *et al.* Morbidity and mortality of major pulmonary resections in patients with early-stage lung cancer: initial results of the randomized, prospective ACOSOG Z0030 trial. *The Annals of thoracic surgery* **81**, 1013–1019, discussion 1019–1020, <https://doi.org/10.1016/j.athoracsur.2005.06.066> (2006).
14. Watanabe, S. *et al.* Should mediastinal nodal dissection be routinely undertaken in patients with peripheral small-sized (2 cm or less) lung cancer? Retrospective analysis of 225 patients. *European journal of cardio-thoracic surgery: official journal of the European Association for Cardio-thoracic Surgery* **20**, 1007–1011 (2001).
15. Wang, L. *et al.* Lymph node metastasis in clinical stage IA peripheral lung cancer. *Lung Cancer* **90**, 41–46, <https://doi.org/10.1016/j.lungcan.2015.07.003> (2015).
16. Matsuguma, H. *et al.* Proportion of ground-glass opacity on high-resolution computed tomography in clinical T1 N0 M0 adenocarcinoma of the lung: A predictor of lymph node metastasis. *The Journal of thoracic and cardiovascular surgery* **124**, 278–284 (2002).
17. Cho, S., Song, I. H., Yang, H. C., Kim, K. & Jheon, S. Predictive factors for node metastasis in patients with clinical stage I non-small cell lung cancer. *The Annals of thoracic surgery* **96**, 239–245, <https://doi.org/10.1016/j.athoracsur.2013.03.050> (2013).
18. Koike, T., Koike, T., Yamato, Y., Yoshiya, K. & Toyabe, S. Predictive risk factors for mediastinal lymph node metastasis in clinical stage IA non-small-cell lung cancer patients. *Journal of thoracic oncology: official publication of the International Association for the Study of Lung Cancer* **7**, 1246–1251, <https://doi.org/10.1097/JTO.0b013e31825871de> (2012).
19. Travis, W. D. *et al.* International association for the study of lung cancer/american thoracic society/european respiratory society international multidisciplinary classification of lung adenocarcinoma. *Journal of thoracic oncology: official publication of the International Association for the Study of Lung Cancer* **6**, 244–285, <https://doi.org/10.1097/JTO.0b013e318206a221> (2011).
20. Sica, G. *et al.* A grading system of lung adenocarcinomas based on histologic pattern is predictive of disease recurrence in stage I tumors. *The American journal of surgical pathology* **34**, 1155–1162, <https://doi.org/10.1097/PAS.0b013e3181e4ee32> (2010).
21. Russell, P. A. *et al.* Does lung adenocarcinoma subtype predict patient survival?: A clinicopathologic study based on the new International Association for the Study of Lung Cancer/American Thoracic Society/European Respiratory Society international multidisciplinary lung adenocarcinoma classification. *Journal of thoracic oncology: official publication of the International Association for the Study of Lung Cancer* **6**, 1496–1504, <https://doi.org/10.1097/JTO.0b013e318221f701> (2011).
22. Warth, A. *et al.* The novel histologic International Association for the Study of Lung Cancer/American Thoracic Society/European Respiratory Society classification system of lung adenocarcinoma is a stage-independent predictor of survival. *Journal of clinical oncology: official journal of the American Society of Clinical Oncology* **30**, 1438–1446, <https://doi.org/10.1200/JCO.2011.37.2185> (2012).
23. Travis, W. D. *et al.* International Association for the Study of Lung Cancer/American Thoracic Society/European Respiratory Society: international multidisciplinary classification of lung adenocarcinoma: executive summary. *Proceedings of the American Thoracic Society* **8**, 381–385, <https://doi.org/10.1513/pats.201107-042ST> (2011).
24. Rosenkrantz, A. B. *et al.* Clinical utility of quantitative imaging. *Acad Radiol* **22**, 33–49, <https://doi.org/10.1016/j.acra.2014.08.011> (2015).
25. Miyasaka, Y., Suzuki, K., Takamochi, K., Matsunaga, T. & Oh, S. The maximum standardized uptake value of fluorodeoxyglucose positron emission tomography of the primary tumor is a good predictor of pathological nodal involvement in clinical N0 non-small-cell lung cancer. *European journal of cardio-thoracic surgery: official journal of the European Association for Cardio-thoracic Surgery* **44**, 83–87, <https://doi.org/10.1093/ejcts/ezs604> (2013).
26. Koksai, D. *et al.* The correlation of SUVmax with pathological characteristics of primary tumor and the value of Tumor/ Lymph node SUVmax ratio for predicting metastasis to lymph nodes in resected NSCLC patients. *Journal of cardiothoracic surgery* **8**, 63, <https://doi.org/10.1186/1749-8090-8-63> (2013).
27. Li, M. *et al.* Primary tumor PET/CT [(1)(8)F]FDG uptake is an independent predictive factor for regional lymph node metastasis in patients with non-small cell lung cancer. *Cancer imaging: the official publication of the International Cancer Imaging Society* **12**, 566–572, <https://doi.org/10.1102/1470-7330.2012.0040> (2013).
28. Hansell, D. M. *et al.* Fleischner Society: glossary of terms for thoracic imaging. *Radiology* **246**, 697–722, <https://doi.org/10.1148/radiol.2462070712> (2008).
29. Onn, A. *et al.* Tumor cavitation in stage I non-small cell lung cancer: epidermal growth factor receptor expression and prediction of poor outcome. *Radiology* **237**, 342–347, <https://doi.org/10.1148/radiol.2371041650> (2005).
30. Zhang, L. *et al.* Three-dimensional computerized quantification for lung invasive adenocarcinoma with different histopathological subtypes in clinical stage I. *Chinese Journal of Radiology* **49**, 268–272 (2015).
31. Yoshizawa, A. *et al.* Validation of the IASLC/ATS/ERS lung adenocarcinoma classification for prognosis and association with EGFR and KRAS gene mutations: analysis of 440 Japanese patients. *Journal of thoracic oncology: official publication of the International Association for the Study of Lung Cancer* **8**, 52–61, <https://doi.org/10.1097/JTO.0b013e3182769aa8> (2013).
32. Gu, J. *et al.* Prognostic significance of the IASLC/ATS/ERS classification in Chinese patients-A single institution retrospective study of 292 lung adenocarcinoma. *Journal of surgical oncology* **107**, 474–480, <https://doi.org/10.1002/jso.23259> (2013).
33. Woo, T. *et al.* Prognostic value of the IASLC/ATS/ERS classification of lung adenocarcinoma in stage I disease of Japanese cases. *Pathology international* **62**, 785–791, <https://doi.org/10.1111/pin.12016> (2012).
34. Takahashi, M. *et al.* Tumor invasiveness as defined by the newly proposed IASLC/ATS/ERS classification has prognostic significance for pathologic stage IA lung adenocarcinoma and can be predicted by radiologic parameters. *The Journal of thoracic and cardiovascular surgery* **147**, 54–59, <https://doi.org/10.1016/j.jtcvs.2013.08.058> (2014).

Acknowledgements

This work was supported by National Natural Science Foundation of China (Grant No. 81601494) and PUMC Youth Fund and the Fundamental Research Funds for the Central Universities (Grant No. 3332016030, 2017320017). The funding source had no involvement in study design, interpretation of data and in the writing of the article.

Author Contributions

N.W. conceived/designed the study and guaranteed the integrity of entire study. M.L. contributed to literature review and writing of the manuscript. L.Z. was responsible for research management, data collection and interpretation. J.W. and L.L. contributed to radiological data collection. W.S. and D.L. contributed to confirmation of pathology. J.R. contributed to statistic analysis.

Additional Information

Supplementary information accompanies this paper at <https://doi.org/10.1038/s41598-017-16701-x>.

Competing Interests: The authors declare that they have no competing interests.

Publisher's note: Springer Nature remains neutral with regard to jurisdictional claims in published maps and institutional affiliations.



Open Access This article is licensed under a Creative Commons Attribution 4.0 International License, which permits use, sharing, adaptation, distribution and reproduction in any medium or format, as long as you give appropriate credit to the original author(s) and the source, provide a link to the Creative Commons license, and indicate if changes were made. The images or other third party material in this article are included in the article's Creative Commons license, unless indicated otherwise in a credit line to the material. If material is not included in the article's Creative Commons license and your intended use is not permitted by statutory regulation or exceeds the permitted use, you will need to obtain permission directly from the copyright holder. To view a copy of this license, visit <http://creativecommons.org/licenses/by/4.0/>.

© The Author(s) 2017